Toward Precision Physics Test with CEνNS Cryogenic COHERENT CsI detectors

R. Pavarani([1])

([1]) *Istituto Nazionale di Fisica Nucleare (INFN), Sezione di Cagliari, Complesso Universitario di Monserrato - S.P. per Sestu Km 0.700, 09042 Monserrato (Cagliari), Italy*

Summary. — I present the potential of future COHERENT detectors that use cryogenic cesium iodide to constrain fundamental parameters in electroweak physics. I have performed an analysis of the precision that can be achieved in measuring several Standard Model (SM) parameters, such as the Weinberg angle, the neutron distribution radii of iodine and cesium, and the neutrino charge radius. I also discuss the potential for probing new physics models involving electromagnetic properties of neutrinos, as predicted by certain theories beyond the SM.

1. – Introduction

Coherent elastic neutrino-nucleus scattering (CEνNS) occurs when a low energy neutrino scatters off an atomic nucleus as a whole via the weak neutral current with the initial and final states of the nuclear target being indistinguishable. CEνNS was first observed by the COHERENT experiment at the Spallation Neutron Source (SNS) using a CsI[Na] scintillator detector [1], 43 years after it was predicted [2]. This breakthrough opened a new avenue to study weak interaction parameters, nuclear form factors, and neutrino properties beyond the Standard Model (SM). A key experimental challenge in observing CEνNS is the small momentum transfer, which makes detection difficult. This highlights the significance of the COHERENT experiment's achievement for astrophysics, nuclear physics, and particle physics. The energy of neutrinos from a stopped pion neutron source (tens of MeV) is ideally suited for CEνNS studies, as they yield sufficiently high scattering rates and nuclear recoil energies above detector thresholds. In this work I present the expected sensitivity to key nuclear physics parameters such as the neutron root mean square (rms) radius of cesium and iodine nuclei, fundamental SM quantities, including the weak mixing angle, and the neutrino charge radius, as well as potential signatures of neutrino properties predicted by theories beyond the SM (BSM), using the two upcoming COHERENT detectors: COH-Cryo-CsI-I and COH-Cryo-CsI-II. The COHERENT program is closely linked to the ongoing upgrades at the SNS. In the near future, the SNS proton beam energy will increase from 1.01 GeV to

1.3 GeV and the beam power will rise to 2 MW. As a result, the number of neutrinos per flavor produced for each proton-on-target will increase to a value of 0.123 [18], which is the value adopted for our sensitivity studies. A second target station is planned for the 2030s, with a final power of 2.8 MW, significantly increasing the neutrino flux for each neutrino flavor compared to the current configuration. Our sensitivity study focuses on the 10 kg COH-CryoCsI I and the following 700 kg COH-CryoCsI II cryogenic CsI detectors, which will be installed at different times. For this reason I assume a 2 MW beam power for COH-CryoCsI I and a 2.8 MW beam power for COH-CryoCsI II in our analysis. For this work, I assume a light yield of 50 PE/keV$_{\text{ee}}$ for both COH-CryoCsI I and COH-CryoCsI II, which represent the highest measurement obtained in several tests performed by the COHERENT collaboration [19]. This value is significantly higher then the 13.35 PE/keV$_{\text{ee}}$ achieved by the COHERENT CsI detector, primarily due to the transition from PMTs to silicon photomultipliers (SiPMs). The SiPMs enable more efficient light collection thanks to their quantum efficiency of approximately 50% [20]. The behavior of the energy efficiency near the threshold is not well known, as no direct measurement is available. To account for this uncertainty, I set the threshold using a stepping function to 0.8 keV$_{\text{nr}}$, i.e. 6 PE, based on the expectation that the acceptance plateau will be reached in that region. These conservative assumptions mitigate potential uncertainties in the knowledge of the acceptance shape near the threshold. It is also extremely important to assume nuclear quenching required for calculating the CEνNS signal prediction. Generally, only a fraction of the energy deposited by a recoiling nucleus produces scintillation light, much is lost due to ionization and heat. Though data analysis is underway, preliminary estimates point to a roughly energy independent quenching factor of $15 \pm 1.5\%$ as reported in Ref. [19]. The COHERENT collaboration is currently developing a detailed background model which includes events from intrinsic rates, afterglow effects in the detector, and external sources, by means of extensive simulations [19]. Notably, the new detector, operating at cryogenic temperatures, is expected to achieve a lower background level compared to the CsI detector. Thanks to its low-threshold, increased light yield and enhanced quenching factor, a signal to background ratio < 1 is expected such that the sensitivities are not strongly dependent on the actual background rate. For simplicity, I will consider an optimistic background-free experiment as I verified that I are able to reproduce the results reported in Ref. [19] for some benchmark models.

2. – Theoretical framework

The CEνNS differential cross section as a function of nuclear recoil energy T_{nr} for a neutrino $\nu_l (l = e, \mu, \tau)$ scattering off a nucleus N with Z protons and N neutrons is [3]:

$$\frac{d\sigma_{\nu_l - \mathcal{N}}}{dT_{\text{nr}}} = \frac{G_{\text{F}}^2 M}{\pi} \left(1 - \frac{M T_{\text{nr}}}{2E^2}\right) (Q_{l,\text{SM}}^{\text{V}})^2, \tag{1}$$

where G_{F} is the Fermi constant, E the neutrino energy, M the nuclear mass and the weak nuclear charge is

$$Q_{l,\text{SM}}^{V} = [g_{\text{V}}^{p}(\nu_l) Z F_Z(|\vec{q}|^2) + g_{\text{V}}^{n} N F_N(|\vec{q}|^2)]. \tag{2}$$

I indicate with F_{Z} and F_{N} the proton and neutron form factors of the nucleus and with g_{V}^{n} and g_{V}^{p} the coefficients which quantify the weak neutral-current interactions of neutrons and protons. The flavor dependence of $g_{\mathrm{V}}^{p}(\nu_l)$ is due to the neutrino charge radii (CR), which represent the only non-zero electromagnetic properties of neutrinos in the SM [4]. The SM neutrino CR prediction can be written as [5, 6]

$$\langle r_{\nu_l}^2 \rangle_{\mathrm{SM}} = -\frac{G_{\mathrm{F}}}{2\sqrt{2}\pi^2}\left[3 - 2\ln\left(\frac{m_l^2}{m_{\mathrm{W}}^2}\right)\right], \tag{3}$$

where m_{W} is the W boson mass, m_l is the mass of the charged lepton $l = e, \mu, \tau$. The SM values of the neutrino CR of interest for this work are:

$$\langle r_{\nu_e}^2 \rangle_{\mathrm{SM}} \simeq -0.83 \times 10^{-32}\mathrm{cm}^2 \tag{4a}$$

$$\langle r_{\nu_\mu}^2 \rangle_{\mathrm{SM}} \simeq -0.48 \times 10^{-32}\mathrm{cm}^2. \tag{4b}$$

The proton, $F_{\mathrm{Z}}(|\vec{q}|^2)$, and neutron, $F_{\mathrm{N}}(|\vec{q}|^2)$, nuclear form factors (FFs) in Eq.(2) encode the dependence of the process on the nuclear structure, and are defined as the Fourier transform of the corresponding nucleon density distributions in the nucleus, $\rho_{\mathrm{Z(N)}}$, respectively. Their effect becomes more relevant for increasing momentum transfers, $|\vec{q}|^2 \simeq \sqrt{2MT_{\mathrm{nr}}}$ [7] leading to a suppression of the full coherence [8] in the CEνNS process.

The SM cross section for neutrino-electron elastic scattering (νES) off an atom $\mathcal{A}$ is

$$\frac{d\sigma_{\nu_\ell-\mathcal{A}}}{dT_{\mathrm{e}}} = Z_{\mathrm{eff}}^{\mathcal{A}}\frac{G_{\mathrm{F}}^2 m_e}{2\pi}\left[(g_{\mathrm{V}}^{\nu_\ell} + g_{\mathrm{A}}^{\nu_\ell})^2 + (g_{\mathrm{V}}^{\nu_\ell} - g_{\mathrm{A}}^{\nu_\ell})^2\left(1 - \frac{T_e}{E}\right)^2 - \left((g_{\mathrm{V}}^{\nu_\ell})^2 - (g_{\mathrm{A}}^{\nu_\ell})^2\right)\frac{m_e T_e}{E^2}\right], \tag{5}$$

where m_e is the electron mass, T_e is the electron recoil energy, and the flavor-dependent couplings are

$$g_{\mathrm{V}}^{\nu_e} = 0.9524, \quad g_{\mathrm{A}}^{\nu_e} = 0.4938, \tag{6a}$$

$$g_{\mathrm{V}}^{\nu_\mu} = -0.0394, \quad g_{\mathrm{A}}^{\nu_{\mu,\tau}} = -0.5062, \tag{6b}$$

when including also radiative corrections [9, 10] and the latest weak mixing angle calculation [11]. For antineutrinos, $g_{\mathrm{A}} \to -g_{\mathrm{A}}$.

The factor $Z_{\mathrm{eff}}^{\mathcal{A}}$ accounts for the number of electrons ionized at a given recoil energy T_e, correcting the cross section derived under the Free Electron Approximation (FEA), which assumes free, stationary electrons [12]. Values of $Z_{\mathrm{eff}}^{\mathcal{A}}$ for Cs and I are provided in Ref. [13]. In certain BSM scenarios, the νES contribution could increase significantly, making it important to investigate this opportunity. Indeed, stronger constraints can be obtained on many neutrino electromagnetic properties [13, 14, 15, 16, 17].

3. – Results

For my sensitivity studies, I adopt the Asimov dataset to evaluate the test statistic using the most-likely dataset, which yields the median of the test statistic. To evaluate the statistical constraints on the parameters, I perform a χ^2 analysis, taking into account both the energy and time distributions. This allows to search for deviations from what

I consider the best description of the physics. To construct the fit of the weak mixing angle, the radius was fixed to $R_n(\text{CsI}) = 5.06$ fm [21] allowing $\sin^2\theta_\text{W}$ to vary in constant steps around its reference value. By calculating the χ^2 for each point, I identify the χ^2_min, which defines the best-fit point and thus the value that best matches the data. Obvioulsy in the sensitivity analysis, this corresponds to the SM prediction. The results are shown in figure 1. For both detectors, COH-CryoCsI I and COH-CryoCsI II, I estimate that the uncertainty will be reduced by a factor of 5 with respect to the first CsI detector.

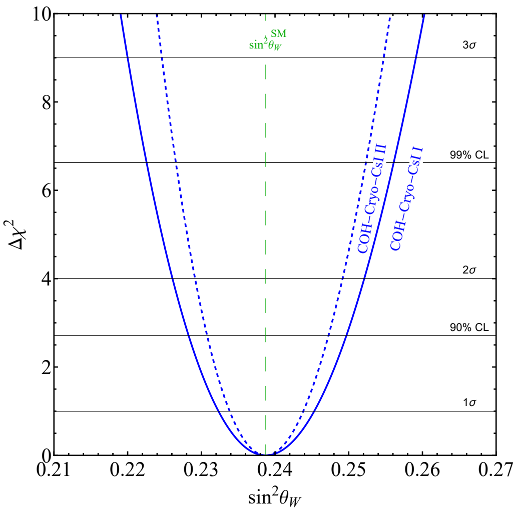

Fig. 1. – Constraints on the weak mixing angle at different confidence levels from the analysis of COH-CryoCsI I and COH-CryoCsI II detectors.

In the same way, the weak mixing angle was fixed to the SM value, $\sin^2\theta_\text{W} = 0.23873$ [11], in order to fit $R_n(\text{CsI})$ in fig. 2. In this case, according to my sensitivity analysis, the uncertainty is expected to reduce by a factor of 2 for COH-CryoCsI I and by a factor of 15 for COH-CryoCsI II. It is clear that reducing systematic uncertainties is crucial to improving the weak mixing angle precision. On the other hand, achieving a more precise measurement the nuclear neutron radius primarily requires increased statistics.

Using the same χ^2 analysis, I also fit the neutrino charge radius. The results are promising when compared to those from the first CsI detector. The new measurements should constrain the allowed region to values close to the SM prediction, whereas the previous measurement identified four possible regions at the 90% of confidence level, for both electron and muon neutrinos [22]. The detection of CEνNS also allows us to place constraints on properties predicted by BSM theories, such as the neutrino magnetic moment and millicharge. With the new COH-CryoCsI I and COH-CryoCsI II detectors, I expect to reach a constraint on magnetic moment at the level of $10^{-10}\,\mu_B$ which is very close to the best current limits for both ν_e and ν_μ. Similarly, the constraint on the millicharge is expected to be of the order of $10^{-11}\,e_0$ also approaching the current best limits [9].

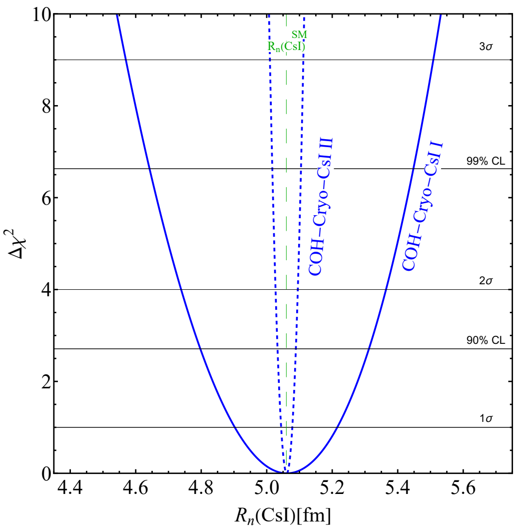

Fig. 2. – Constraints on the nuclear neutron radius at different confidence levels from the analysis of COH-CryoCsI I and COH-CryoCsI II detectors.

4. – Conclusion

The upcoming COH-CryoCsI I and COH-CryoCsI II detectors from the COHERENT collaboration are expected to significantly improve the precision of key electroweak and nuclear measurements through CEνNS. In this study, I have shown that they will enable a fivefold improvement in the measurement of the weak mixing angle and a substantial enhancement in the determination of the nuclear neutron radius. The new detectors will also strongly constrain the neutrino charge radius and allow competitive limits on electromagnetic properties such as the neutrino magnetic moment and millicharge, approaching the best existing bounds. These results highlight the crucial role of COH-CryoCsI detectors in future precision tests of the SM and searches for new physics.

REFERENCES

[1] D. Akimov et al., *SCIENCE*, **357** (2017) 1123
[2] D. Z. Freedman, *Phys. Rev. D*, **9** (1974) 1389
[3] M. Cadeddu et al, *EPL*, **143** (2023) 34001
[4] C. Giunti et al, *arXiv:2411.03122* , (2024)
[5] J. Bernabéu et al, *Phys. Rev. D*, **62** (2000) 113012
[6] J. Bernabéu et al, *Phys. Rev. Lett.*, **89** (2002) 229902
[7] M. Cadeddu et al, *Phys. Rev. Lett.*, **120** (2018) 072501
[8] M. Atzori Corona et al., *Eur. Phys. J. C*, **83** (2023) 683
[9] M. Cadeddu et al, *Phys. Rev. D*, **107** (2023) 053001
[10] J. Erler and S. Su, *Prog. Part. Nucl. Phys.*, **71** (2013) 119
[11] Navas, S. et al., *Phys. Rev. D*, **110** (2024) 030001
[12] Kouzakov et al., *Adv. High Energy Phys.*, **1** (2014) 569409
[13] M. Atzori Corona et al., *JHEP*, **09** (2022) 164
[14] P. Coloma et al., *JHEP*, **05** (2022) 037
[15] M. Agostini et al., *Phys. Rev. D*, **96** (2017) 091103

[16] O. G. Miranda et al., *Phys. Rev. B*, **808** (2020) 135685
[17] W. Grimus et al., *Nucl. Phys. B*, **648** (2003) 376
[18] D. Akimov et al., *American Physical Society*, **106** (2022) 032003
[19] P. S. Barbeau et al., *Phys. Rev. D*, **109** (2024) 092005
[20] C. Jackson et al., *Optical Engineering*, **53** (2014) 081909
[21] M. Hoferichter et al., *Phys. Rev. D*, **102** (2020) 074018
[22] M. Atzori Corona et al., *JHEP*, **05** (2024) 271